

# Experimental study on the failure factors of the O-ring for long-term working<sup>①</sup>

SUN Yuantao(孙远韬)<sup>②\*</sup>, ZHANG Min\*, YUAN Lindong\*\*

(\* School of Mechanical Engineering, Tongji University, Shanghai 200092, P. R. China)

(\*\* Metering Department, Shanghai, Fiorenti Gas Equipment CO., LTD, Shanghai 201201, P. R. China)

## Abstract

The O-ring in the rotary dynamic sealing system of gas meters should have outstanding long-term sealing performance under the conditions of high and low temperature, which can ensure the safety of gas meters. In this paper, based on the O-ring sealing mechanism, taking the compression set as the main sealing index, a finite element simulation method is used to analyze the failure characteristics under different conditions according to the constitutive relation of nitrile rubber. Then, using the orthogonal test method for the O-ring sealing performance index, the main factors which affect the law of long-term test are analysed, and the orthogonal regression mathematical model that can predict the compression set is obtained. Finally, the O-ring is improved according to the model, and the test results show that the performance of the new O-rings with high and low temperature resistance is greatly improved and meets the expected target requirements.

**Key words:** NBR O-ring, compression set, rotary dynamic seal, orthogonal test, regression analysis

## 0 Introduction

O-ring is suitable for a variety of mechanical equipment, and can play a sealing role in a static or moving state in specified temperatures, pressure, and different liquid and gas media. It is widely used in machine tools, ships, automobiles, aerospace equipment, machineries in industries, and various of instruments and meters. As the core component in the sealing system, once the O-ring fails, the light will lead to sealing media leakage, equipment can not work properly or even cause serious accidents.

For gas meters, in order to ensure the accuracy of measurement and gas safety, the long-term sealing method of gas meters must be reliable. Among several mainstream gas meters sealing methods, the O-ring seal is the most widely used one. Nitrile rubber (hereinafter referred to as NBR) is the most common O-ring material due to its good mechanical properties, resistance to lubricants and grease, and relatively low cost<sup>[1]</sup>. It is valuable to study the long-lasting sealing performance of the sealing system of the NBR O-ring rotary dynamic sealing system for gas meters, both from the perspective

of safe gas use and life time requirements.

In terms of O-ring failure indicators, Ref. [2] conducted long-term tests of O-rings to predict the service life of packages used for long-term cross section, to reduce strain energy, and monitoring of storage, and their preliminary data suggests that CSR (compressive stress relaxation) data are valuable for predicting the service life of O-rings when there is no leakage. Ref. [3] studied the dynamic and static sealing performance of O-rings using a specially designed test device, and concluded that the O-ring compression set can be used as an important index to evaluate its sealing performance.

For O-ring dynamic sealing performance studies, Ref. [4] predicted the life and reliability of O-rings by non-destructive tests (e. g. Shore a hardness measurements) and used them to aid decision making. A two-dimensional axisymmetric computational fluid dynamics (CFD) model was preprocessed in GAMBIT of Ref. [5], and heat transfer analysis was performed using FLUENT to investigate the variation of frictional torque, O-ring frictional power loss, and interface temperature with sliding velocity and operating differential pressure. The results show that the power loss of the O-

① Supported by the National Key Research and Development Program of China (No. 2018YFC0808902).

② To whom correspondence should be addressed. E-mail: sun1979@sina.com.

Received on Sep. 22, 2022

ring increases roughly linearly with the increase in sliding speed<sup>[5]</sup>. Ref. [6] investigated the design of O-ring cross-sections, which include small embedded regions with different material behavior among the surrounding large the compression set, and time-varying load deformation behavior of the specimens showed that the amount of compression set is related to the strain energy, while the compression set of the material affects the performance of the structure. Ref. [7] performed rapid measurements of various parameters affecting the dynamic performance of O-rings, including O-ring stiffness and damping coefficient, through test procedures. In order to investigate the effects of extrusion and pressure on the dynamic properties of NBR and fluorocarbon O-rings, tests were conducted and it was concluded that increasing the level of extrusion or system pressure increased the stiffness and damping coefficient, as well as the size of the O-ring cross-sectional diameter had little effect on the stiffness and damping coefficient. Ref. [8] studied the performance of O-ring reciprocating dynamic seals in hydraulic systems and analyzed the effect of different stresses and design parameters on contact pressure with finite element software to obtain the degree of influence of applied stresses and seal structure design parameters on the sealing performance of O-rings.

For the selection of test methods, Ref. [9] designed a procedure applicable to the characterization of deformation behavior of various engineering materials during processing. The procedure used orthogonal processing tests to obtain the relationships between shear stress, strain, strain rate, and temperature. A novel constitutive model for mild steel determined by this procedure was proposed with the help of the orthogonal test method. Ref. [10] used the orthogonal experimental method to reduce the number of experiments and determine the key parameters in the relevant experiments, and divided the nine parameters into three groups, including printing parameters, temperature parameters and structural parameters. The three groups of experiments were investigated separately to determine the effects of factors on the mechanical properties of shape memory polymer (SMP) samples, and the optimal combination of temperature and printing parameters for SMP printing and the effect of structural parameters on the tensile strength of the specimens were determined. This experimental study involves three factors and three levels, in order to better analyze the effects of time, rotational speed and temperature on the compression set of the sealing index and its corresponding sealing effect, and because the time of this experimental study is too long, this paper will design the orthogonal test

with three factors of time, temperature and rotational speed for the study, which can greatly shorten the test time and at the same time ensure the validity of the test results.

In summary, at present, research on the sealing performance of NBR O-ring in sealing system mainly focuses on the O-ring itself (such as aging index, static sealing performance, dynamic sealing performance) and the performance of NBR original material (such as material life, intrinsic model selection), and lacks a comprehensive research analysis combining simulation and actual life cycle test on the O-ring rotary dynamic sealing system from the perspective of sealing failure factors<sup>[11-14]</sup>. In this paper, the failure characteristics of the O-ring is analyzed under different working conditions by using the finite element simulation method based on the intrinsic structure relationship of nitrile rubber for the compression set, and on this basis, we conduct long-term tests and analysis on the sealing performance indexes and the influence law of the main influencing factors of the O-ring by orthogonal test method, and obtain the orthogonal regression mathematical model that can predict the compression set and finally improve the O-ring according to this model.

## 1 NBR O-ring rotary dynamic sealing system finite element analysis

### 1.1 Introduction to structure of the O-ring sealing system

As shown in Fig. 1, the rotary sealing system consists of an O-ring, a split washer, a linkage shaft, a linkage bushing, and a linkage shaft seat, with the O-ring near the split washer side being the inside of the meter body, i. e., the side that bears the pressure of the medium, and the other side being the outside of the meter body. The gap between the linkage shaft and the linkage shaft seat is sealed in both directions by the O-ring, isolating the inside of the meter body from the outside of the meter. During the ventilation work, the male crank drives the linkage flag to rotate, thus making the linkage shaft rotate and transfer the gas volume to the counter to meter.

Among the main causes of O-ring failure in sealing systems<sup>[15]</sup>, the reduction of seal overflow caused by the compression set is an important cause of seal failure<sup>[3]</sup>, and at the same time, the compression set can be observed and measured visually, qualitatively and quantitatively, so this paper selects the index of the compression set of the O-ring to study its sealing performance.

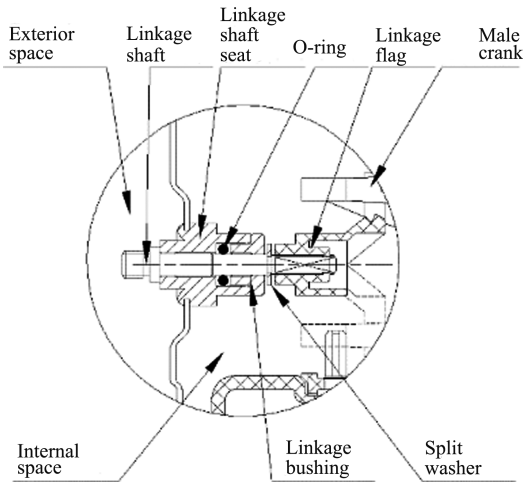


**Fig. 1** O-ring rotary dynamic sealing system structure diagram

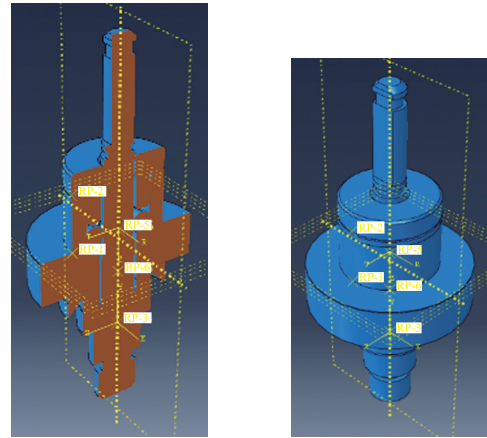
The O-ring is mainly subjected to shear stress, contact stress and Von Mises stress in the sealing system, which lead to compression set. Therefore, the effect of temperature and rotational speed on these three forces can reflect the effect of temperature and rotational speed on the compression set of O-rings to a certain extent. Considering that the mechanical results in ABAQUS are more accurate and easier to obtain than the compression set, the above three forces are chosen to represent the compression set to a certain extent in the simulation experiment.

This finite element analysis which is established a finite element model in ABAQUS, according to the simulation experimental protocol, through the analysis of the above three stresses under different working conditions, can obtain the results of the force of the O-ring in the sealing system under the composite factors and meanwhile deduce the degree of influence of each factor alone on the O-ring in the sealing system, thus to predict the possible compression permanent deformation area<sup>[16-18]</sup>.

The Mooney-Rivlin model has been validated for finite element mechanical analysis of rubber materials, especially for small and medium deformations, and is a good fit for the O-ring in this study. The calculated deformation, damage and other failure forms of the O-ring during the simulated stress analysis of the O-ring sealing system will be closer to the actual test results<sup>[19-21]</sup>. The 3D model of the rotating dynamic sealing system in this study is modeled using SOLIDWORKS, the 3D model is simplified in ABAQUS, which is easy to converge the simulation results, as shown in Fig. 2; the 3D stress linear cell C3D8R is used to mesh the model in ABAQUS<sup>[22-25]</sup>, the established O-ring model is shown in Fig. 3.

Other pre-processing steps of FEA are as follows: (1) Set the pre-compression of O-ring to 15%<sup>[26]</sup>;

(2) Set the temperature field according to the working condition; (3) Apply 2 kPa working medium pressure to the seal to complete the static sealing process; (4) Apply two reverse rotational velocities to the shaft barrel to simulate the rotational motion process, and the velocity size will be changed according to the working condition.



(a) Section view (b) Overall assembly view

**Fig. 2** ABAQUS simplified model diagram

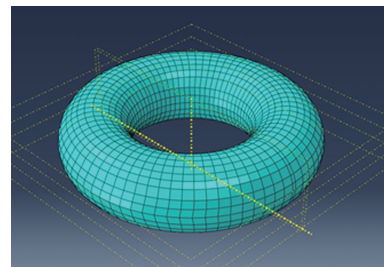


**Fig. 3** Drawing of the 3D O-ring mesh model

The simulation test factors are temperature, rotational speed and pressure. The operating pressure is fixed at 2 kPa, and the temperature is set as  $-25\text{ }^{\circ}\text{C}$ ,  $20\text{ }^{\circ}\text{C}$  and  $60\text{ }^{\circ}\text{C}$ ; according to the working principle of the membrane gas meter used in this study, the rotational speed is 86 r/min when the gas flow rate  $q = 6\text{ m}^2/\text{h}$ , and 58 r/min when  $q = 4\text{ m}^2/\text{h}$ , so the test rotational speed is 86 r/min, 58 r/min and 0 r/min. The two-factor, three-level full-scale experimental protocol for temperature and speed is shown in Table 1.

Table 1 Two-factor, three-level full-scale experimental protocol

RPM	Temperature		
	B1 ( $-25\text{ }^{\circ}\text{C}$ )	B2 ( $20\text{ }^{\circ}\text{C}$ )	B3 ( $60\text{ }^{\circ}\text{C}$ )
A1 (86 r/min)	A1B1	A1B2	A1B3
A2 (58 r/min)	A2B1	A2B2	A2B3
A3 (0)	A3B1	A3B2	A3B3

### 1.2 Simulation experiment results and data analysis

Simulation analysis was performed for each of the nine scenarios according to Table 1. ABAQUS was applied to set up the load scenarios by experimental protocol, and numerical simulations were performed to analyze and output force clouds and data as required<sup>[27-30]</sup>, where the results of Scenario 1 are shown in Fig. 4, and the results of the other eight scenarios are shown in Appendix I ( limited to space ).

(1) A comparison of the average Von Mises stress data for the nine scenarios is shown in Fig. 5. From Fig. 5, it can be seen that the Von Mises stress of the O-ring and does not vary much increases with increasing temperature in the dynamic seal state; the stress value does not vary much at different rotational speeds; in the static seal state, does not vary much with decreasing temperature. The Von Mises stress is not sensitive to temperature, does not vary much between different rotational speeds, and varies greatly between dynamic and static.

(2) A comparison of the average contact stress data for the nine scenarios is shown in Fig. 6. As can be seen from Fig. 6, the contact stress of the O-ring, which increases with temperature, varies greatly; the stress values at different rotational speeds are relatively close and do not vary much. Contact stress is more sensitive to temperature and has a good effect; the speed has a relatively small effect on contact stress.

(3) The average shear stress data comparison is shown in Fig. 7. As can be seen from Fig. 7, the shear stress CSHEAR 1 and CSHEAR 2 of the O-ring, increases with temperature in the dynamic seal condition; in the static seal condition, the stress decreases with temperature and both vary greatly. The difference in stress values between dynamic and static seals is large, and the stress values at different rotational speeds are relatively close and do not vary much. Shear stress is more sensitive to temperature and has a significant effect; rotational speed has a relatively small effect on contact stress.

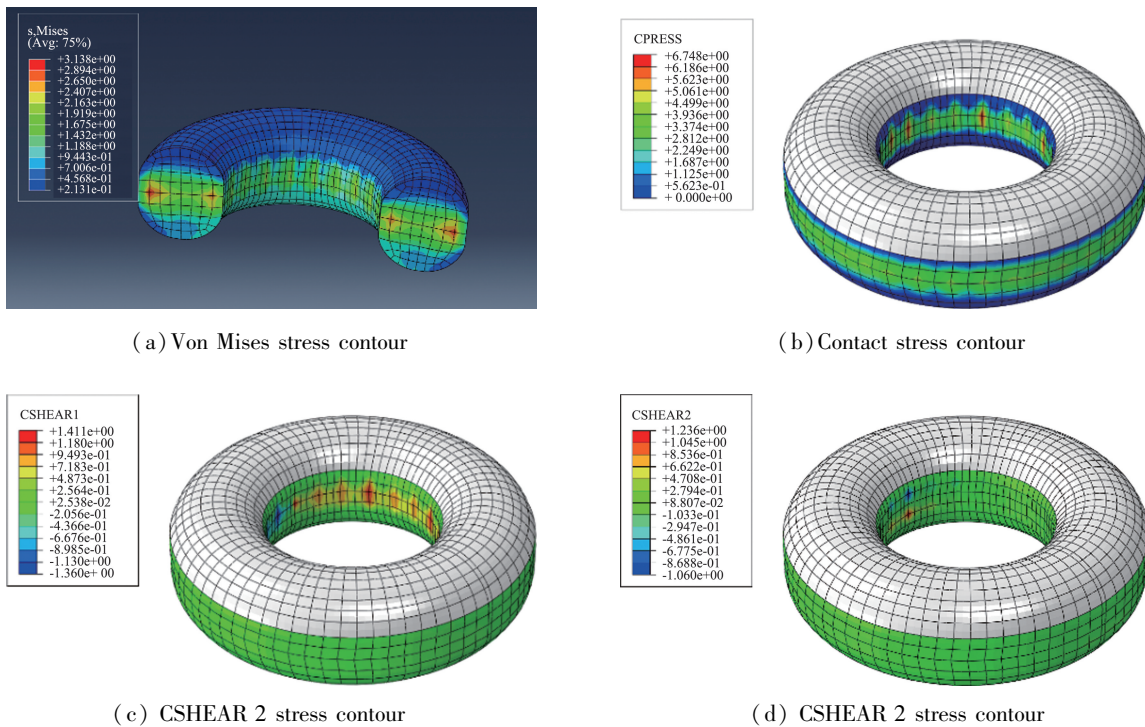


**Fig. 4** Scenario 1: A1B1 ( test conditions : -25 °C , 86 r/min , 2 kPa )

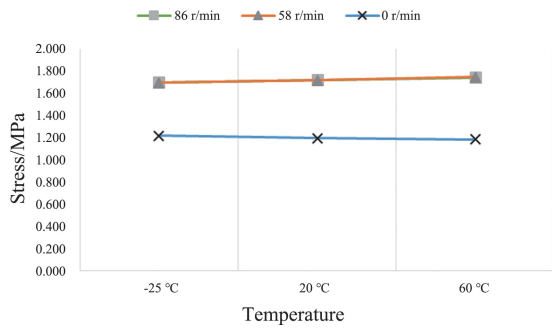


Fig. 5 Average Von Mises stress comparison

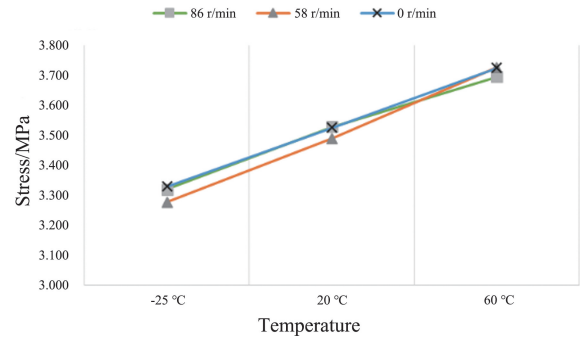
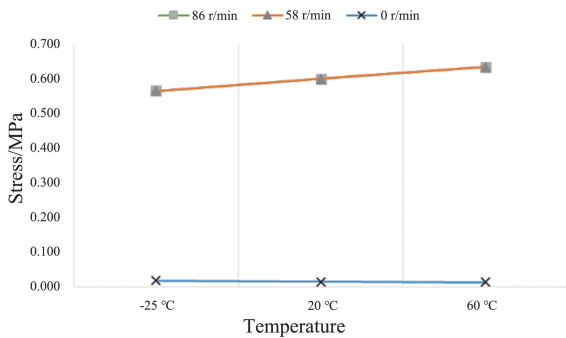
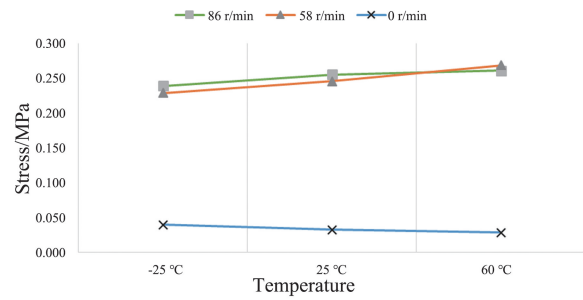


Fig. 6 Average contact stress comparison



(a) CSHEAR 1 comparison



(b) CSHEAR 2 comparison

Fig. 7 Average shear stress comparison

Through finite element analysis, the results of the influence of temperature and rotational speed on the three stresses were obtained as follows.

(1) Von Mises stresses vary little at different temperatures (the maximum of variation is at 58 r/min; 3%), the response is not obvious; contact stresses and shear stresses vary much at different temperatures (contact stresses: 13.73% at 58 r/min; CSHEAR1: -22.29% at 0 r/min; CSHEAR2: -28.36% at 0 r/min), the response is obvious.

(2) Von Mises stresses, contact stresses and shear stresses vary little at different speeds under dynamic seal condition (Von Mises stresses: 0.0143% at 20 °C; Contact stresses: 0.0154% at -25 °C; CSHEAR 1: 0.00357% at 20 °C; CSHEAR 2: 0.0392% at -25 °C), the response is not obvious.

(3) Whether the seal state is static or not has a significant effect on Von Mises stresses and shear stresses, while it is not significant for contact stresses. And because the permanent compression deformation of O-ring depends on the above three stresses, it can be seen that the temperature has the greatest influence on the sealing performance of O-ring, followed by the speed.

## 2 Experimental study of the NBR O-ring rotary dynamic sealing system

In this test, air was used as the medium for the ventilation and sealing test to simulate as much as possible the conditions of the O-ring during the actual operation of the gas meter. At the end of the test, an underwater devices for detecting seal ability was used to test that if there was no leakage within 1 min<sup>[31]</sup>, the O-ring sealing performance was considered to meet the requirements. The O-ring that completed the test was taken out and its dimensions were measured and the data were analyzed and the compression set  $C_f \leq 50\%$  at -25 °C, 20 °C and  $C_f \leq 40\%$  at 60 °C were considered to meet the requirements, and vice versa<sup>[29]</sup>.

The compression set measurement method is based on ISO 815-1<sup>[32]</sup>, and the compression set rate is calculated by Eq. (1) to quantitatively evaluate the amount of compression set as follows.

$$C_f = \frac{d_0 - d_f}{d_0 - d_c} \times 100\% \quad (1)$$

where  $C_f$  is amount of compression set of the O-ring in compression,  $d_0$  is O-ring original section diameter,  $d_f$  is O-ring section diameter after the compression, and  $d_c$  is thickness of the O-ring under compression.

## 2.1 Experimental protocol

In the study, the three factors (time, temperature and speed) were set as follows.

(1) Time: 2000 h, 3500 h, 6000 h

2000 h and 3500 h are the stage tests in the 5000 h endurance test, and at the same time, 2000 h is the minimum endurance test requirement to be met by the gas meter; the upper limit of 6000 h is selected to have higher performance requirements for the sealing system, while the interval range covers 5000 h, so that the model obtained from the test can cover the range of 2000 h to 6000 h.

(2) Temperature:  $-25\text{ }^{\circ}\text{C}$ ,  $20\text{ }^{\circ}\text{C}$ ,  $60\text{ }^{\circ}\text{C}$

$20\text{ }^{\circ}\text{C}$  is the room temperature;  $-25\text{ }^{\circ}\text{C}$  and  $60\text{ }^{\circ}\text{C}$  are the higher requirements for high and low temperature working environment of gas meters.

(3) Speed: 86 r/min, 58 r/min, 0 r/min

The maximum flow rate of the gas meter is  $6\text{ m}^3/\text{h}$ , which corresponds to the rotational speed of 86 r/min; the most common flow rate of the gas meter is  $4\text{ m}^3/\text{h}$ , which corresponds to the rotational speed of 58 r/min, and the state of rotational speed of 0 r/min under 0 flow rate.

The orthogonal test protocol is shown in Table 2<sup>[33-34]</sup>.

Table 2 Table of three-factor, three-level test protocol (L9(3<sup>3</sup>))

Num	Factors		
	Time/h	Temperature/ $^{\circ}\text{C}$	RPM
1	2000	$-25$	58
2	2000	20	86
3	2000	60	0
4	3500	60	86
5	3500	20	58
6	3500	$-25$	0
7	6000	20	0
8	6000	$-25$	58
9	6000	60	86

There are 9 groups of tests, and each group needs to test 6 gas meters, i. e. 6 O-rings.

## 2.2 Test environment and equipment

(1) Test environment

Temperature:  $20 \pm 2\text{ }^{\circ}\text{C}$ ;

Relative humidity: 35% – 75% RH;

Atmospheric pressure: 86 – 106 kPa;

Medium: air.

(2) Testing device

1) Endurance test device: it consists of profile bracket, speed control fan, pipeline and gas meter,

where each fan drives two gas meters, the flow rate is controlled by the speed of rotation of the roller counter in gas meter, regulating the actual flow rate of  $6\text{ m}^3/\text{h}$  (86 r/min),  $4\text{ m}^3/\text{h}$  (58 r/min). The working principle of the endurance device is shown in Fig. 8.

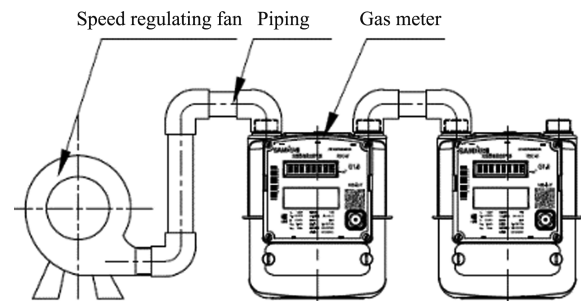


Fig. 8 Schematic of the endurance test device

2) Gas meter sealing testing device: it is made up of gas pipeline, pressure gauge, cylinder, lifting mechanism, water tank. Test pressure can be adjusted by turning the knob manually.

3) Digital projector, high- and low-temperature test chamber, experimental meters, etc., see Appendix II for details.

## 2.3 Results of the orthogonal test

After completing 9 scenarios in accordance with the orthogonal test protocol, the performance of the O-ring rotary dynamic sealing system was tested by the water test method with the seal testing device; after the test, the O-ring sealing system sealing test was all qualified, and in terms of the test O-ring, the O-ring long-term sealing performance was proved to be reliable. The testing process is shown in Fig. 9.

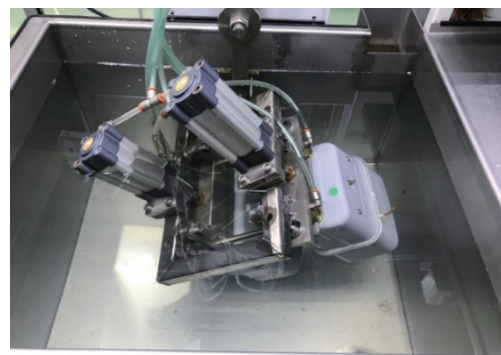


Fig. 9 Diagram of the gas meter sealing test process

After the experiments were completed, six gas meters in each of the nine groups were disassembled, the deformed O-rings were removed, and their section diameters and overall internal diameters were measured using a projector. It was found that the O-rings had ob-

vious compression set in the radial direction by compression. Before data processing, the section diameters and overall inner diameters of the six O-rings of the same batch that were not used were measured in advance as initial values. After obtaining the O-ring dimension data, the measured data were handled according to Eq. (1) to obtain the compression set data, and the range  $R$  was calculated according to the three-factor, three-level orthogonal table data processing method, and the test data are shown in Table 3. [35-36]

Table 3 Test results data sheet

Num	Factors			Average compression set
	Time/h	Temperature/ °C	RPM	
1	2000	-25	58	44.81%
2	2000	20	86	20.83%
3	2000	60	0	23.43%
4	3500	60	86	39.50%
5	3500	20	58	21.48%
6	3500	-25	0	27.91%
7	6000	20	0	16.28%
8	6000	-25	58	61.29%
9	6000	60	86	56.22%
$K_1$	0.8907	1.3401	1.1655	
$K_2$	0.8889	0.5859	1.2758	
$K_3$	1.3379	1.1915	0.6762	
$k_1$	0.2969	0.4467	0.3885	
$k_2$	0.2963	0.1953	0.4253	
$k_3$	0.4460	0.3972	0.2254	
range $R$	0.1497	0.2514	0.1999	

2.3.1 Intuitive analysis method

To distinguish the primary and secondary factors of the test, as well as to determine the significance of the influence of each factor on the test indexes, intuitive analysis was first used to obtain the results as shown in Fig. 10 based on the data in Table 3.

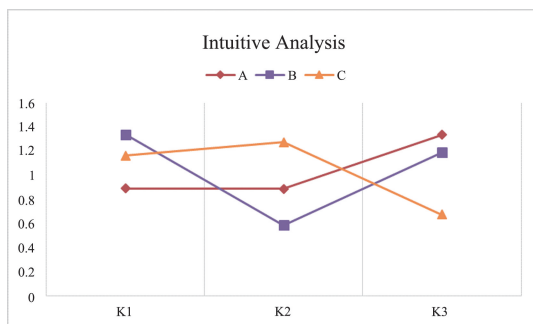


Fig. 10 Intuitive analysis

From Fig. 10, it can be intuitively seen that the

value of the largest range of variation is factor  $B$ , factor  $C$  ranks second, and factor  $A$  is the most inferior, so it can be judged that the degree of influence of these three factors on the compression set of compression is: factor  $B > \text{factor } C > \text{factor } A$ , that is, the temperature factor has the greatest influence, followed by the speed factor, and the time factor has the least influence.

2.3.2 Analysis of variance (ANOVA) method

To obtain more precise analysis results, the data was then further processed by ANOVA to obtain the degree of significance of the effects of different factors. The experimental data were calculated using a three-factor ANOVA using the Matlab ANOVA formula [37-40], and the results are shown in Table 4, where,  $SS$  is variance,  $D_f$  is degree of freedom,  $MS$  is mean squared error,  $F$  denotes F-value, and  $Prob > F$  denotes P-value.

Table 4 Results of the ANOVA calculation

Source	$SS$	$D_f$	$MS$	$F$	$Prob > F$
Factor $A$	0.044 62	2	0.022 31	80.50	0.0123
Factor $B$	0.104 42	2	0.252 21	188.37	0.0053
Factor $C$	0.065 91	2	0.032 96	118.91	0.0083
Error	0.000 55	2	0.000 28		
Sum	0.217 49	8			

The F-test was performed on the ANOVA, and from Table 4, it can be concluded that the P-values of factor  $B$ , and factor  $C$  are less than 0.01, and both reject the  $H_0$  hypothesis, so both factors have a significant effect on the compression set at  $\alpha = 0.01$  significance level; and since the P-value of factor  $B$  is smaller, so between the two factors, factor  $B$  has a greater effect and factor  $C$  is the second. The effect of factor  $A$  was not significant at  $\alpha = 0.01$  significance level. That is, among the three factors, temperature has the greatest effect on compression set, rotational speed is the second and time is the third. This conclusion is consistent with the results obtained from the previous finite element simulation and the two can corroborate each other.

2.4 Orthogonal fit regression analysis of experimental data

To maximize the effect of the results of this test, regression analysis was performed on the compression set data to obtain a prediction model of the relationship between three factors: time, temperature, rotational speed, and the compression set of the O-ring. To facilitate the calculation of the whole data analysis process, before proceeding to analyze the data, the data were processed in advance using normalization methods to avoid the problem of inconsistent physical meaning of each data parameter [41-43]. The following quadratic poly-

nomial response model for the fitted and estimated amounts of compressive compression set, Eq. (2) is developed.

$$y = a + b_1x_1 + b_2x_2 + b_3x_3 + b_4x_1x_2 + b_5x_2x_3 + b_6x_1x_3 + b_7x_1^2 + b_8x_2^2 + b_9x_3^2 + \varepsilon \quad (2)$$

where,  $x_1$  denotes time factor  $A$ ;  $x_2$  denotes temperature factor  $B$ ;  $x_3$  denotes speed factor  $C$ ;  $a$  denotes the constant term;  $b_1 - b_3$  denotes the primary term coefficients;  $b_4 - b_9$  denotes the secondary term coefficients;  $\varepsilon$  denotes the model error.

The data in Table 2 are normalized by using Matlab and substituted into Eq. (2) together with the data in Table 3 for compression set, and the response model coefficients are solved by least squares method with the help of Matlab<sup>[44-45]</sup>, and the quadratic polynomial response model Eq. (3) for the compression set target can be obtained by substituting the normalized model coefficient values into Eq. (1).

$$y = 0.2016 + 0.0887x_1 - 0.0481x_2 + 0.1155x_3 + 0.0145x_1x_2 + 0.0234x_2x_3 - 0.0548x_1x_3 + 0.0095x_1^2 + 0.2119x_2^2 \quad (3)$$

## 2.5 Model fitting accuracy test and prediction test validation

### 2.5.1 Model fitting accuracy test

The coefficient of determination  $R^2$  is used as the evaluation index model for the accuracy fitting test, which is defined in Eq. (4).

$$R^2 = \frac{SSR}{SST} \quad (4)$$

where  $SSR$  denotes the regression sum of squares of response estimates and response means, see Eq. (5);  $SST$  denotes the sum of squares of total deviations of response values and response means, see Eq. (6).

$$SSR = \sum_{i=1}^N (\hat{y}_i - \bar{y})^2 \quad (5)$$

$$SST = \sum_{i=1}^N (\hat{y}_i - \bar{y})^2 \quad (6)$$

where  $N$  denotes the number of trials,  $I$  denotes the  $i$ th trial,  $\hat{y}_i$  denotes the response function,  $\bar{y}$  denotes the mean value of  $N$  trials,  $\hat{y}_i$  denotes the test result<sup>[46]</sup>.

$R^2 = 0.8840$ , which exceeds 0.8, shows that the model fits well and that this compression permanent variable response model has high accuracy.

### 2.5.2 Test verification

The prediction model of the compression set of O-ring was tested and verified; according to the same conditions of the previous orthogonal test, a group (6 units) of gas meters was arranged, the time was set to 5000 h, the temperature was 20 °C, and the speed was

86 r/min. After the test was completed, the O-ring samples were taken out, their dimensions were measured with a projector, and the data were obtained and calculated according to Eq. (1). Their average compression set was 30.89%, which was compared with the predicted value of 33.61% given by the normalized quadratic polynomial prediction model, and the error value was 8.81%, indicating that the results of the prediction model had a small error value with the test data, and the relative accuracy was high.

## 3 NBR O-ring rotary dynamic seal performance improvement and application

The previous experimental study verified that the sealing performance of the O-ring met the requirements, but by Table 5, it can be seen that: dynamic sealing system O-ring in -25 °C low temperature state, after 2000 h of continuous work, its compression set value reached 44.81%, close to 50%; after 6000 h of continuous work, the compression set value reached 61.29%, more than 50%, the indicator does not meet the requirements; dynamic sealing system O-ring in 60 °C high temperature state, after 3500 h of continuous work, its compression set value reached 39.50%, close to 40%; after 6000 h of continuous work, the compression set value reached 56.22%, more than 40%, the indicator does not meet the requirements either. To allow the O-ring to work properly under high and low temperatures for a long time and to ensure that its sealing performance meets the requirements, the O-ring performance is targeted to be improved.

After several rounds of communication with the technical engineers of the Italian joint venture company and the O-ring manufacturer, it was considered that the most important thing was to improve the performance of O-rings at high and low temperatures. However, since -25 °C is close to the low temperature resistance limit of NBR material, based on the standard durability requirements of the product<sup>[47]</sup>, and at the same time, considering the cost of modification and the cost factor of mass production, it was finally decided to set the modified endurance test time of O-ring at high and low temperature as 5000 h, and the following experiments are designed to verify the rationality of the change, and the experimental protocol is shown in Table 5.

After normalizing the parameters of the two test scenarios in Table 5 and substituting them into Eq. (3), the predicted average compression set value of the original O-ring at 5000 h can be obtained, as shown in the last column of Table 5.

Table 5 Validation experimental protocol

Number	Factors			Compression set
	Time/h	Temperature/ °C	RPM	
1	5000	-25	86	56.58%
2	5000	60	86	53.09%

For the modified O-ring samples, the original dimensions were measured, and some samples were selected to prepare 2 sets of gas meters for testing. According to the modification target, the test time was selected as 5000 h, and high- and low-temperature endurance tests were conducted to verify them. After testing, all tested O-rings rotating dynamic sealing system are not leaking, and the sealing test results meet the requirements of compliance.

The two sets of meters with the required sealing performance were disassembled, and the test O-rings were removed and stored separately according to the group. Measure the size of the O-ring and calculate according to Eq. (1) to obtain the compressive compression set of the two sets of O-rings, as shown in Table 6.

Table 6 Verification test results table

Number	Factors			Average compression set	Required average compression set
	Time/h	Temperature / °C	RPM		
1	5000	-25	86	42.60%	50%
2	5000	60	86	36.68%	40%

From Table 6, it can be obtained that the compressive compression set index of modified O-rings was significantly improved. For Scenario 1, the average compression set value of the deflection of the O-ring is 42.30%, which is less than 50%. For Scenario 2, the average compressive compression set value of the O-rings is 36.68%, which is less than 40%. The compressive compression set of the O-rings under high and low temperatures meet the requirements, and the improvement has been successful.

The compression set values obtained from the test are compared with the data of the original O-ring obtained according to the prediction model, and the comparison of compression set before and after improvement is obtained in Table 7.

Table 7 Comparison of the compression set before and after modification

Number	Compression set after modification	Compression set before modification	Improvement ratio
1	42.30%	56.58%	25.24%
2	36.68%	53.09%	30.91%

The average compression set value was reduced by 25.24% for Scenario 1 and by 30.91% for Scenario 2. According to the comparison between the test value of compression set and the calculated value, the new O-ring sample has been greatly improved compared with the existing O-ring products in terms of comprehensive performance of high and low temperature resistance and wear resistance, and the improvement range is 25% - 30%, which is very satisfactory. Finally, the product was tested and put into commercial use, and good results were achieved, which proved that the research results of this study were reasonable and effective.

## 4 Conclusions

Based on the characteristics of gas meters with long service life, wide temperature range and large differences in flow specifications, this paper focuses on the influence of three factors, namely time, temperature and speed, on the sealing performance of O-rings for research and analysis. Based on the fact that compression set is an important index for O-ring performance evaluation and its advantage of being visually observed and measured, it is chosen as the evaluation index for O-ring performance in this study. The orthogonal experimental protocol was reasonably designed and multiple experiments were conducted accordingly, and the experimental data were analyzed visually and by ANOVA, the qualitative degree of influence of three main factors on the compression set index was obtained: the temperature factor had the greatest influence, followed by the rotational speed factor, and the time factor had the least influence. After that, regression analysis was carried out on the experimental data to derive the quantitative relationship between the compression set and the three factors, and finally, corresponding experiments were arranged to verify the validity and precision of the relationship.

Through the analysis of the sealing mechanism of the rotary dynamic sealing system, the finite element simulation analysis of the O-rings in the sealing system, and the empirical study of the orthogonal test, the theory and practice are combined to complete the study of the O-ring rotary dynamic sealing system. And according to the conclusion of the study, the O-ring is modified and optimized as well as further experimental verification. The difficulty of this study lies mainly in the simulation and test part; during the simulation process, O-ring as a nonlinear elastomer, has the characteristics of difficulty of converging the simulation results, especially this test needs to load composite factors, the convergence of results is more difficult; during

the test process, the biggest difficulty was the long test time, which accumulated to 49 500 h, using a large amount of equipment resources and test materials.

### Nomenclature

$C_f$	Amount of compression set of the O-ring in compression
$d_0$	O-ring original section diameter
$d_f$	O-ring section diameter after compression
$d_c$	Thickness of the O-ring under compression
$SS$	Variance
$D_f$	Degrees of freedom
$MS$	Mean squared error
$F$	F-value
$Prob > F$	P-value
$R$	Range
$x_1$	Time factor $A$
$x_2$	Temperature factor $B$
$x_3$	Speed factor $C$
$a$	Constant term
$b_1 - b_3$	Primary term coefficients
$b_4 - b_9$	Secondary term coefficients
$\varepsilon$	The model error
$R^2$	Coefficient of determination
$\hat{y}_i$	Response function
$\bar{y}$	Mean value of $N$ trials
$y_i$	Test result

### References

- [1] BAI C, YU S C, LIU H Y, et al. Wear failure mechanism and surface carbon film modification technology of nitrile rubber [J]. Flight Control and Detection, 2202, 5(1): 92-102.
- [2] HOFFMAN E N, SKIDMORE T E, DAUGHERTY W L. Long-term leak tightness of O-ring seals in the 9975 shipping package [C] // Proceedings of the ASME 2010 Pressure Vessels and Piping Division/K-PVP Conference. Bellevue: ASME, 2010: 433-438.
- [3] SHAO T M. Influence of compression set on the sealing performance of O-ring [J]. Lubrication Engineering, 1997 (4): 47-49.
- [4] FRIGIONE M, RODRÍGUEZ-PRÍETO A. Can accelerated aging procedures predict the long term behavior of polymers exposed to different environments? [J]. Polymers, 2021, 13 (16): 2688.
- [5] LINGERKAR K, KHONSARI M M. On the effects of sliding velocity and operating pressure differential in rotary O-ring seals [J]. Institution of Mechanical Engineers, Journal of Engineering Tribology, 2010, 224(7): 649-657.
- [6] MACIEJEWSKI NI, SEFKOW R B, KLAMECKI B E. Composite structure design of O-rings using material behavior to decrease strain energy and permanent deformation [J]. Journal of Tribology, 2009, 131(4): 042202.
- [7] ITZHAK G, CAPEL E. Analysis of elastomeric O-ring seals in compression using the finite element method [J]. Tribology Transactions, 1992, 35(1): 83-88.
- [8] CHEN J D, XIE Q, WANG Z, et al. Analysis of dynamic sealing characteristics of O-ring in hydraulic valve system [J]. Lubrication Engineering, 2014, 39(11): 63-68.
- [9] LEI S, SHIN Y, INCROPERA F. Material constitutive modeling under high strain rates and temperatures through orthogonal machining tests [J]. Journal of Manufacturing Science and Engineering, 1999, 121(4): 577-585.
- [10] LIU B, YANG L, ZHOU R, et al. Effect of process parameters on mechanical properties of additive manufactured SMP structures based on FDM [J]. Materials Testing, 2022, 64(3): 378-390.
- [11] ZHAO H M, HAN N. Finite element analysis of rotating dynamic seal structure under dynamic pressure [J]. Modern Manufacturing Engineering, 2014, 10: 81-85.
- [12] GU D S, TU Q A, SUN J J, et al. Experimental study on the sealing performance of nitrile rubber O-rings [J]. Lubrication Engineering, 2015, 40(8): 71-75.
- [13] LI W, MAY S. Material and finite element analysis of poly(tetrafluoroethylene) rotary seals [J]. Plastics, Rubber and Composites, 2002, 31(8): 356-363.
- [14] NIKAS G K. Eighty years of research on hydraulic reciprocating seals; review of tribological studies and related topics since the 1930s [J]. Proceedings of the Institution of Mechanical Engineers, Part J: Journal of Engineering Tribology, 2010, 224(1): 1-23.
- [15] DAI X Y, LEI X P. Analysis of failure causes of Buna-N O-ring [J]. Rubber Science and Technology, 2020, 18(1): 17-22. (In Chinese)
- [16] ZHOU C L, ZHENG J Y, GU C H, et al. Sealing performance analysis of rubber O-ring in high-pressure gaseous hydrogen based on finite element method [J]. International Journal of Hydrogen Energy, 2017, 42(16): 11996-12004.
- [17] LI Z C. Research on fatigue life analysis and optimization methods of rubber elastic components [D]. Zhuzhou: Hunan University of Technology, 2015. (In Chinese)
- [18] QIQO L N, CHRISTIAN K, Zencker U, et al. Three-dimensional finite element analysis of O-ring metal seals considering varying material properties and different seal diameters [J]. International Journal of Pressure Vessels and Piping, 2019, 176: 1-6.
- [19] ZHANG Q, SHI J W, SUO G F, et al. Finite element analysis of rubber materials based on Mooney-Rivlin model

- and Yeoh model [J]. China Synthetic Rubber Industry, 2020,43(6):468-471. (In Chinese)
- [20] YÜKSELER R F. Local and nonlocal buckling of Mooney-Rivlin rods [J]. European Journal of Mechanics (A): Solids,2019,30(78):1-11.
- [21] XIE Y. Analysis of the effect of uncertainty in the intrinsic model and material parameters on the mechanical properties of rubber composites [D]. Foshan: Foshan University,2018. (In Chinese)
- [22] DU P G. Basic principles of finite element meshing [J]. Machinery Design and Manufacture,2000(1):34-36. (In Chinese)
- [23] WANG M Q, ZHU Y M, LIU W X. Research on the application of finite element meshing method [J]. Machinery Design and Manufacture,2004(1):22-24. (In Chinese)
- [24] XIA S L, HE J W. Research on finite element meshing based on engineering applications [J]. Aircraft Design, 2008,28(4):10-13. (In Chinese)
- [25] MA X F. ABAQUS 6.11 Finite Element Analysis [M]. Beijing:Tsinghua University Press,2013. (In Chinese)
- [26] LI M, WANG J. Finite element analysis of O-ring dynamic seal characteristics [J]. Mechanical Science and Technology,2015,34(3):386-392. (In Chinese)
- [27] EDWARD L, STANISŁAW O, WOJCIECH C. Simulation studies on ring upsetting using the ABAQUS software [J]. Technical Transactions,2017,10(10):167-178.
- [28] LIU X X, WANG D C, CHENG P, et al. Simulation and optimization of spring forming wire feeding accuracy based on ABAQUS [J]. Modern Manufacturing Engineering, 2020(12):98-104. (In Chinese)
- [29] TOMASZ D, WIESŁAWA P, MARCIN K, et al. Numerical simulations of progressive hardening by using ABAQUS FEA software [J]. MATEC Web of Conferences,2018,157(2):02007.
- [30] ZHU Y F. Research on analysis methods of explicit dynamics based on ABAQUS [J]. Machinery Design and Manufacture,2015(3):107-109,113. (In Chinese)
- [31] State Administration for Market Regulation. Membrane gas meter; GB/T 6968-2019 [S]. Beijing: China Quality and Standards Publishing and Media,2019. (In Chinese)
- [32] International Organization for Standardization. Rubber, vulcanized or thermoplastic; determination of compression set: Part 1: at ambient or elevated temperatures: ISO 815-1:2014 [S]. Switzerland: ISO Copyright Office, 2014.
- [33] MAO Y Q, PU W H, ZHANG H, et al. Orthogonal experimental design of an axial flow cyclone separator [J]. Chemical Engineering and Processing-Process Intensification,2019,144:107645.
- [34] FENG J J, YIN G N S, LIU Z, et al. Uniaxial compression dynamic mechanical properties test of steel-plastic hybrid fiber recycled concrete [J]. Acta Materiae Compositae Sinica,2022,38(11):5386-5402. (In Chinese)
- [35] JENNIFER S. Orthogonal designs [M]. Cham: Springer, 2017.
- [36] WEN C F, HU Q P. Orthogonal test design to optimize on ammonium removal by pseudomonas stutzeri ZH-1 [J]. Journal of Applied Life Sciences International, 2017, 10(2):1-7.
- [37] GUO P. Application of three-way ANOVA with interaction effects and MATLAB implementation [J]. Journal of Shenyang University (Natural Science), 2019, 31(3):252-256. (In Chinese)
- [38] YU G Y, WU H J, ZHANG E D, et al. Matlab concise example tutorial [M]. Nanjing: Southeast University Press, 2016. (In Chinese)
- [39] WANG H, LU G, LU Y C, et al. Application of matlab data processing system in research of drug microemulsion [J]. Advanced Materials Research, 2014, 887-888:623-626.
- [40] ZHANG L, GUO L Y, CONG B. The practical textbook of Matlab [M]. Beijing: Posts and Telegram Press, 2014. (In Chinese)
- [41] NIKOLAOS P. Multiple linear regression analysis [J]. American Journal of Orthodontics and Dentofacial Orthopedics, 2016, 149(4):1-7.
- [42] PARK J, KIM J W, CHANG J H, et al. Estimation of speech absence uncertainty based on multiple linear regression analysis for speech enhancement [J]. Applied Acoustics, 2015, 87: 205-211.
- [43] DIVIA PAUL A, RAMAKRISHNA A, SUBRAMANYAM K. Multiple linear regression analysis for left anterior descending artery (LAD) dimensions for culprit single vessel stenosis in LAD coronary artery [J]. Journal of the Anatomical Society of India, 2018, 67(S1):S37.
- [44] YANG G Y. Mathematical model for air quality data calibration and release with multiple linear regression analysis [J]. China Building Materials Science and Technology, 2020, 29(1):21-23. (In Chinese)
- [45] DONG Q M, SONG T R, JIANG C Y, et al. Application of a multiple linear regression model of FEV1 in pulmonary function test [J]. Journal of Southern Medical University, 2020, 40(12):1799-1803. (In Chinese)
- [46] SUN Y T, YUAN L D, ZHU W Y, et al. Aging study on NBR O-ring in rotary sealing system [J]. Lubrication Engineering, 2020, 45(11):36-40.
- [47] British Standards Institution. Rubber materials for seals and diaphragms for gas appliances and gas equipment: BS EN549-2019 [S]. UK: BSI Standards Limited, 2019.

**Sun Yuantao**, born in 1979. He received his B. S., M. S. and Ph. D degrees from Wuhan LiGong University in 2002, 2005 and 2008, respectively. He is an associate professor in the School of Mechanical Engineering of Tongji University. His research interests include fatigue crack life and correlation analysis of failure modes.

Appendix

I Finite element simulation analysis results of Scenarios 2 to 9

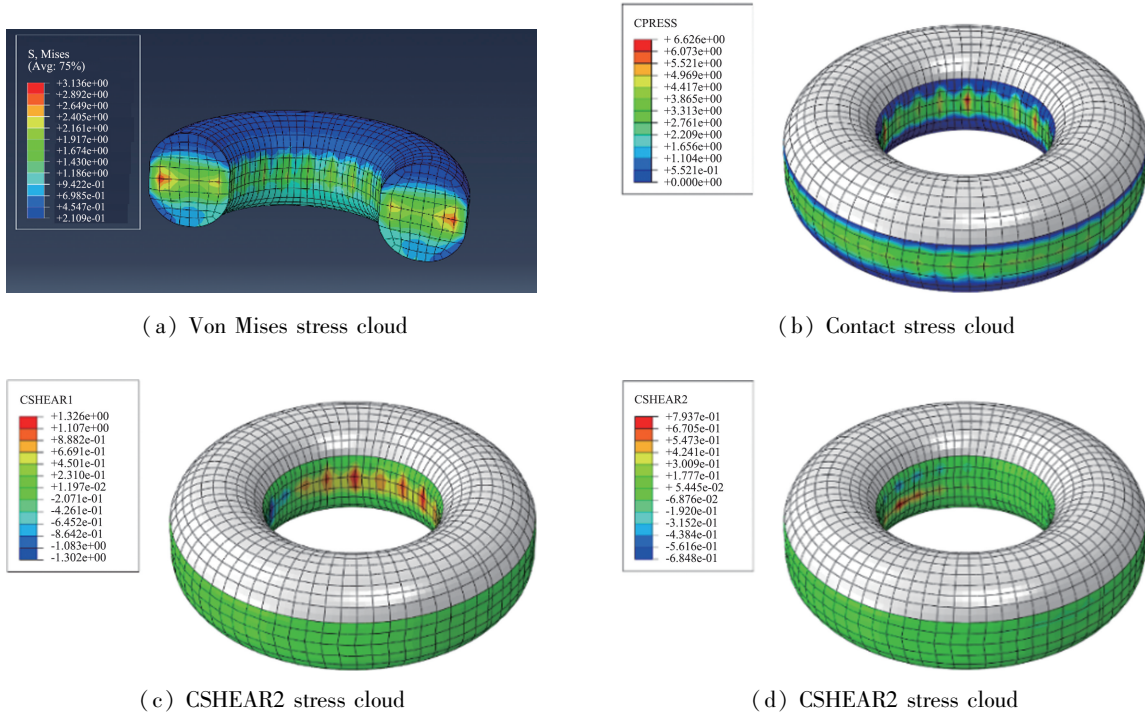


Fig. 11 Scenario 2: A1B2 ( -25 °C , 58 r/min , 2 kPa )

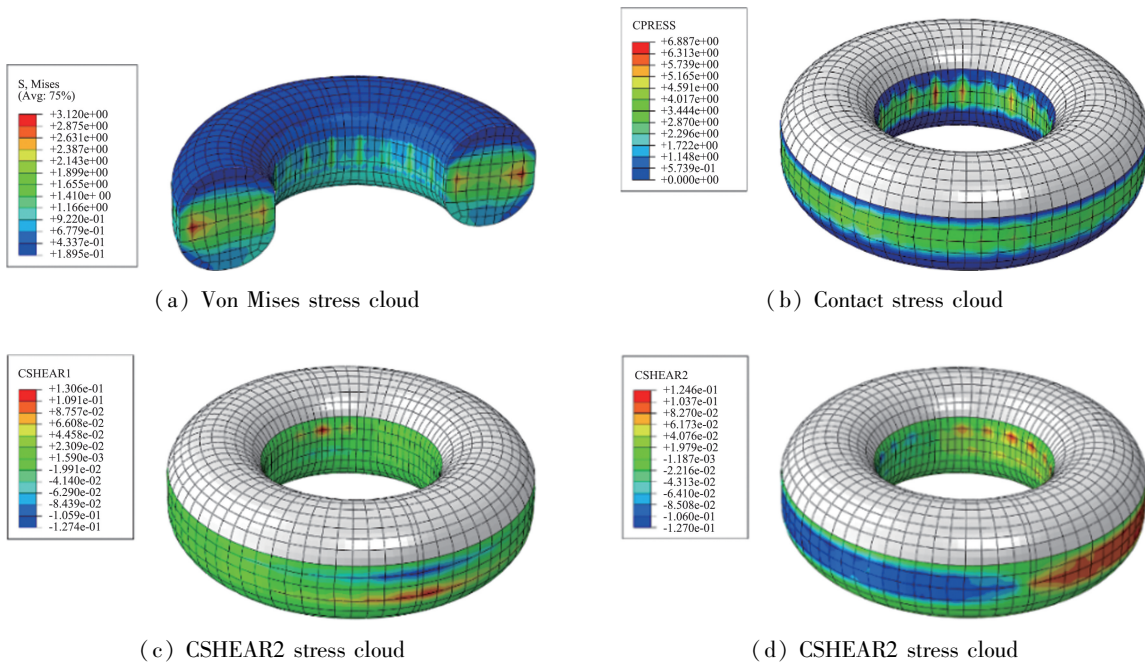
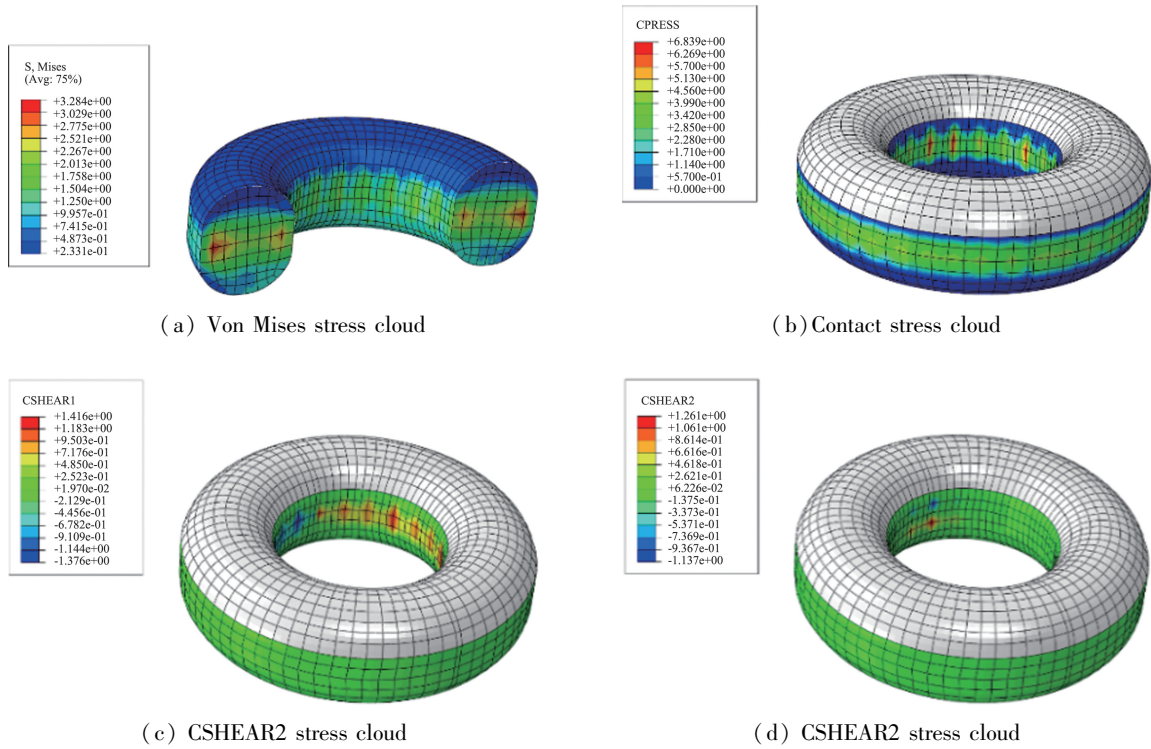
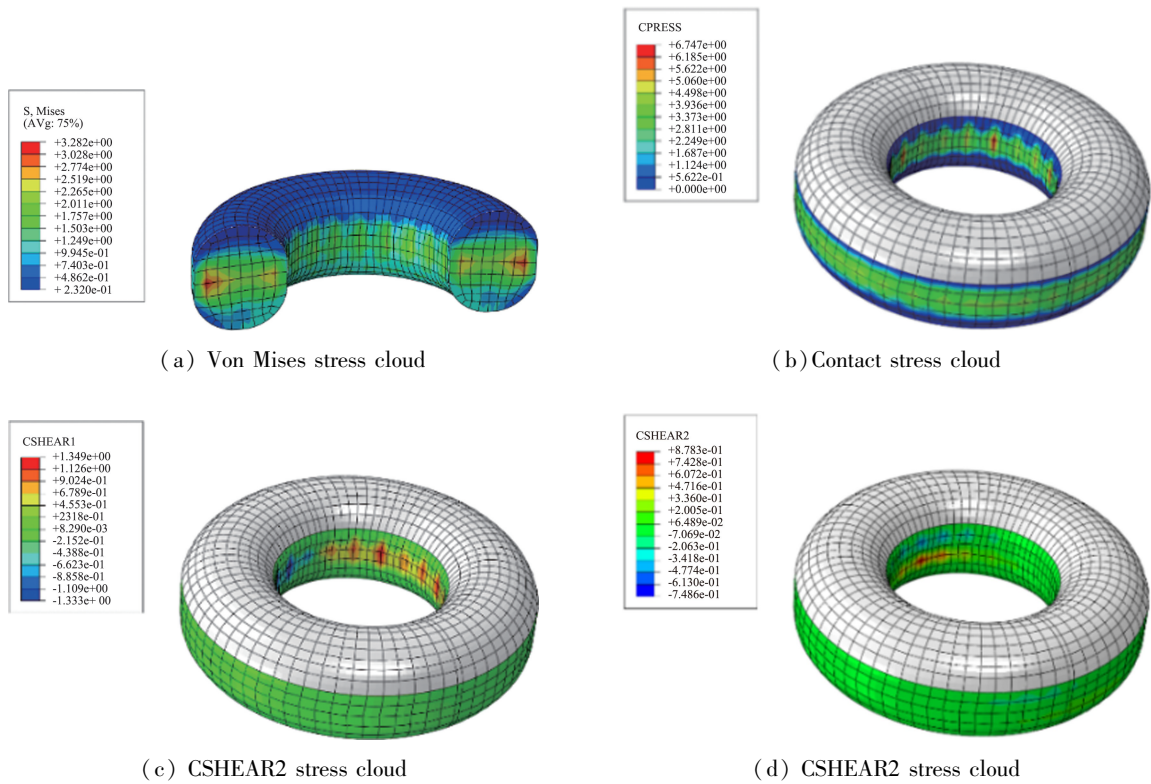


Fig. 12 Scenario 3: A1B3 ( -25 °C , 0 r/min , 2 kPa )



**Fig. 13** Scenario 4: A2B1 (20 °C ,86 r/min,2 kPa)



**Fig. 14** Scenario 5: A2B2 (20 °C ,58 r/min,2 kPa)

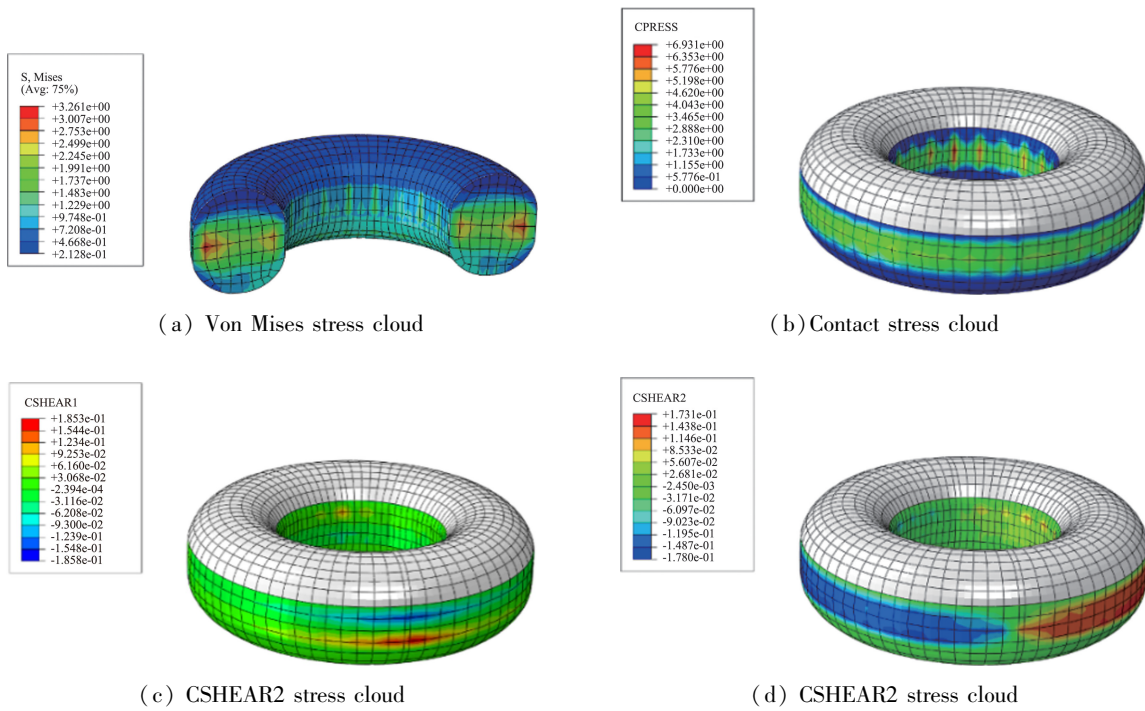


**Fig. 15** Scenario 6: A2B3 ( 20 °C ,0 r/min ,2 kPa)

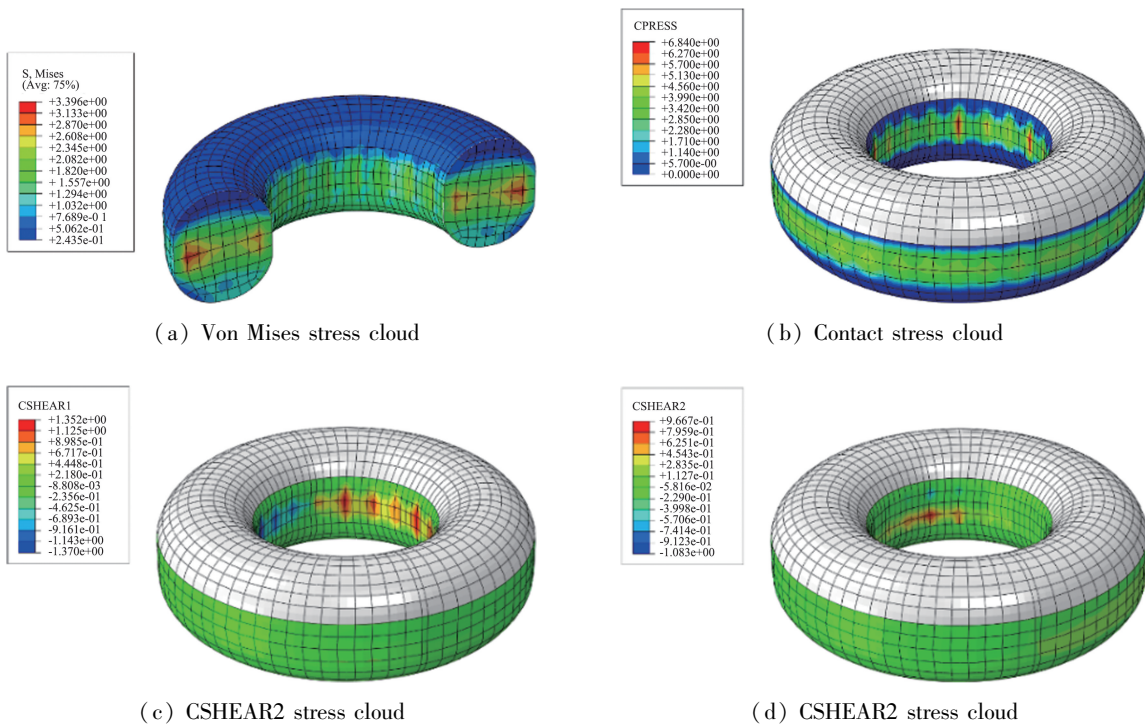


**Fig. 16** Scenario 7: A3B1 (60 °C ,86 r/min ,2 kPa)

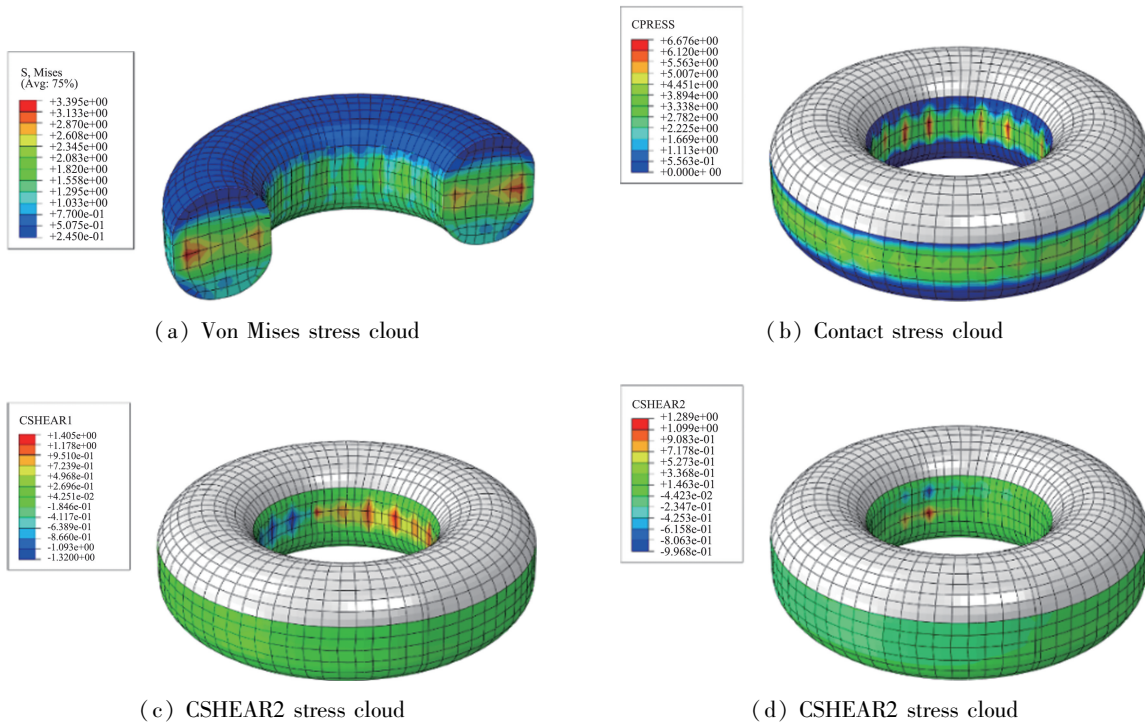


**Fig. 17** Scenario 8: A3B2 (60 °C ,58 r/min,2 kPa)

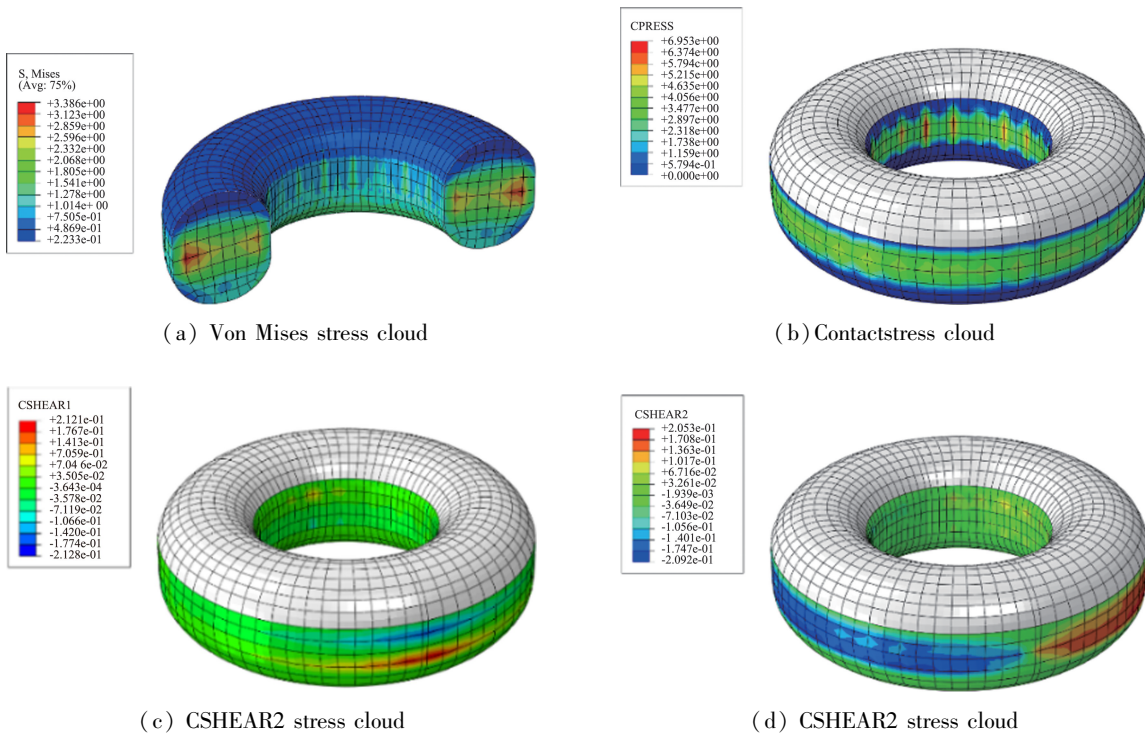


**Fig. 18** Scenario 9: A3B3 (60 °C ,0 r/min,2 kPa)

## II Experimental instruments

(1) Endurance test devices are specially designed and manufactured for this study to test the long-lasting

sealing performance of O-rings in rotary dynamic sealing systems, as shown in Fig. 19.



(a) General endurance test device



(b) High and low temperature endurance testing device

**Fig. 19** Endurance testing device

(2) The gas meter sealing testing device consists of gas line, pressure gauge, cylinder, lifting mechanism and water tank. The test pressure is adjusted by a manual adjustment knob. The device line is readily available and borrowed when testing is required to check the sealing effect of the O-ring rotary dynamic sealing system after endurance testing.

(3) Digital projector: Xintian Optoelectronics JT24  $\Phi$ 300. The shape of the instrument is shown in Fig. 20.

**Fig. 20** Digital projector

(4) High and low temperature test chamber; LINPIN instrument is shown in Fig. 21.

**Fig. 21** High and low temperature test chamber